

Synaptic plasticity alters the nature of chaos transition in neural networks

Wenkang Du¹ and Haiping Huang^{1,2*}

¹*PMI Lab, School of Physics, Sun Yat-sen University,
Guangzhou 510275, People's Republic of China and*

²*Guangdong Provincial Key Laboratory of Magnetoelectric Physics and Devices,
Sun Yat-sen University, Guangzhou 510275, People's Republic of China*

(Dated: December 23, 2024)

Abstract

In realistic neural circuits, both neurons and synapses are coupled in dynamics with separate time scales. The circuit functions are intimately related to these coupled dynamics. However, it remains challenging to understand the intrinsic properties of the coupled dynamics. Here, we develop the neuron-synapse coupled quasi-potential method to demonstrate how learning induces the qualitative change in macroscopic behaviors of recurrent neural networks. We find that under the Hebbian learning, a large Hebbian strength will alter the nature of the chaos transition, from a continuous type to a discontinuous type, where the onset of chaos requires a smaller synaptic gain compared to the non-plastic counterpart network. In addition, our theory predicts that under feedback and homeostatic learning, the location and type of chaos transition are retained, and only the chaotic fluctuation is adjusted. Our theoretical calculations are supported by numerical simulations.

*Electronic address: huanghp7@mail.sysu.edu.cn

I. INTRODUCTION

Revealing mechanisms underlying brain dynamics is one of the most fascinating scientific endeavors of this century. Brain dynamics support our thinking, perception and memory [1, 2], involving two types of coupled dynamic processes—neuronal and synaptic dynamics. The synaptic dynamics control how neurons are non-reciprocally connected, yielding complex neuronal dynamics (e.g., self-organized criticality in neocortex [3]), while the synaptic connections are in turn affected by the evolving neural states (namely synaptic plasticity) [4, 5]. These two sides of brain dynamics complicated all theoretical analyses in previous works [6–8], making a complete understanding of the role of synaptic plasticity still challenging.

Physics has a long history of studying spin dynamics. At a coarse-grained level, the spin state can be treated as a neuronal state. The path integral approach or dynamical mean-field theory was first introduced to study spin dynamics trajectories [9–11] in models where the spin couplings are randomly quenched. However, a later development involved relatively slow dynamics of spin couplings [12, 13], marking an important step both in concepts and techniques towards understanding a complex system of coupled dynamics. On the neural dynamics side, there emerged a lot of theoretical studies about dynamical behaviors of randomly connected neural networks, such as chaos transitions found in high dimensional neural dynamics [14–18], random synapses of low-rank structures [19], and stochastic nonlinear neuronal dynamics with background noises [20]. Recent works started to combine both dynamics in a machine learning system [21, 22], and it was recently addressed how the random untrained and trained parts of the couplings interact to produce expected performances [23], and it was also demonstrated how a Hebbian hierarchy affects retrieval dynamics of memory sequences [24]. In particular, the dynamical mean-field theory was recently used to study the coupled system and reveal that synaptic dynamics can speed up or slow down neuronal dynamics, and thus the chaos can be made freezable (akin to a working memory function) [25]. An intrinsic time scale introduced to Hebbian coupling dynamics leads to the result that older memory and recent memory bear different chaotic temporal fluctuations [26]. Therefore, studying the coupled dynamics based on the dynamical mean-field theory becomes an active scientific frontier in theoretical neuroscience.

The dynamical mean-field analysis would become very complicated in reduced descrip-

tions of the high dimensional coupled dynamics, as partial differential equations need to be solved, which prevents us from studying those complicated scenarios of synaptic and neuronal dynamics and further plasticity-induced phase transitions. Inspired by recent works of quasi-potentials for non-equilibrium neural dynamics [15], we propose a canonical ensemble theory to address the interplay between synaptic plasticity and neural dynamics, focusing only on their zero-speed (or fixed point) limit. We consider three types of commonly used plasticity rules—Hebbian plasticity, random feedback-driven learning, and target rate-oriented homeostatic plasticity, which all bear machine learning benefits [27, 28] and neurobiological relevance [29–32]. Surprisingly, we reveal that the plasticity parameter tunes the nature of the chaos transition from the first order to the second order, which will significantly impact the intrinsic structure of the phase space. We will detail the adopted methodology and discuss the scientific contribution to our understanding of the collective dynamical behavior of the coupled systems.

II. EQUILIBRIUM THEORY OF LEARNING

In this section, we first introduce the recently proposed quasi-potential method for non-gradient neural dynamics, and then describe in detail the proposed framework to treat the theory of learning in this paper. Our framework concentrates on the fixed-point limit of the dynamics, thereby avoiding solving dynamical mean field equations in the traditional path integral framework [33–35]. We shall show the advantage of the quasi-potential method in capturing dynamical phase transitions in this section.

A. Quasi-potential method for non-equilibrium dynamics

We consider a canonical model of an N -neuron coupled recurrent neural network (RNN), where the state of the network is described by the synaptic current $x_i(t) \in \mathbb{R}$. This synaptic current satisfies the following N -dimensional ordinary differential equation:

$$\frac{dx_i}{dt} = -x_i + \sum_{j=1}^N J_{ij} \phi(x_j), \quad (1)$$

where we exclude the self-coupling ($J_{ii} = 0$), the first term on the right-hand side of the equation represents a natural decay in the absence of feedback inputs ($\mathbf{J} = \mathbf{0}$), while the

second term denotes the influence of other neurons j on neuron i , with the non-reciprocal coupling $J_{ij} \neq J_{ji}$. The function ϕ is a nonlinear activation function, which, in this paper, is assumed to be the tanh function by default. Each coupling is generated independently as $J_{ij} \sim \mathcal{N}(0, g^2/N)$, where g captures the strength of synaptic feedback.

The collective dynamical behavior was theoretically clarified in the seminal work [14]. The critical value of $g_c = 1$ separates a trivial null-activity phase from a non-trivial chaotic phase, where two initially close trajectories will finally deviate with a positive rate (called Lyapunov exponent). The chaos transition was recently revealed to have a connection to the concept of topological complexity [16, 17] and peaked response functions at the edge of chaos [15], where the continuous nature of the chaos transition is mathematically justified. We next briefly introduce the quasi-potential method that we shall extend to address the neuronal-synaptic dynamics.

Focusing on the steady fixed-point (may be unstable) state of the non-gradient recurrent dynamics [Eq. (1)], we can intuitively write down the following cost for optimization:

$$E(\mathbf{x}) = \frac{1}{2} \sum_i \left(-x_i + \sum_j J_{ij} \phi(x_j) \right)^2 + \eta \|\mathbf{x}\|^2, \quad (2)$$

where the first term of the energy function represents the kinetic energy (considering the unit mass), while the second term is the regularization term and η is a predefined parameter. This optimization of continuous variables can be done by gradient dynamics with a certain level of white noise whose variance is determined by a temperature T . It is then well known that the steady state of the stochastic gradient dynamics can be described by the Boltzmann distribution [33]:

$$P(\mathbf{x}) = \frac{1}{Z} e^{-\beta E(\mathbf{x})}, \quad (3)$$

where Z is the partition function, \mathbf{x} represents the activity vector, and $\beta = 1/T$. By sending $\beta \rightarrow \infty$, we will immediately arrive at the zero speed limit, i.e., all fixed points (regardless of their stability) can be captured under this Boltzmann measure. This constructs the core idea of the quasi-potential function, i.e., order parameters describing the non-equilibrium dynamics in the zero-speed limit can be obtained from the disorder average over \mathbf{J} , demonstrating that the order can emerge from apparent disorders. Qualitative behavior of the collective dynamics in the long time limit can then be determined by these order parameters. Next, we will develop a theoretical framework to incorporate the effect

of learning on neural dynamics. In other words, our goal is to address a fundamental question of how learning induces the change of the phase space structure underlying the high dimensional chaotic dynamics [8].

B. Canonical ensemble theory of learning

We consider three types of synaptic plasticity rules. The first one is the standard Hebbian type, i.e., the pre-synaptic and post-synaptic neural activities affect the synaptic strength in the following way:

$$J_{ij} = J_{ij}^0 + \frac{k}{N} \phi(x_i) \phi(x_j), \quad (4)$$

where the first term indicates the untrained random substrate (e.g., generating the spontaneously chaotic fluctuations), while the second term explains the local Hebbian effect [29]. The random substrate is a random matrix whose entries are independently generated from $\mathcal{N}\left(0, \frac{g^2}{N}\right)$, and k specifies the strength of the Hebbian term. By varying the value of k , one can see how strongly the Hebbian term affects the steady fixed-point state of the original random RNN.

The second plasticity we consider is the feedback learning [36]. More precisely, in reservoir computing, only a linear readout is trained, and then the output is sent via feedback to all units in the neural reservoir where the coupling is random and untrained (in analogy to \mathbf{J}^0 here). The feedback weight is commonly chosen to be random as well, e.g., following a standard Gaussian distribution. In principle, adding a feedback loop is a highly flexible way of increasing functional adaptability through learning, since nervous systems often seem to be composed of loops [36]. For example, top-down attention may be sent back through this feedback loop. Interestingly, despite unchanged \mathbf{J}^0 , the random feedback amounts to the equivalent rank-one modification of the untrained \mathbf{J}^0 [27], when the readout weight is updated to match the target signal. Therefore, we propose a toy model of this sort of feedback learning.

$$J_{ij} = J_{ij}^0 + \frac{\delta}{N} u_i \phi(x_j), \quad (5)$$

where the constant δ characterizes the feedback strength, and the feedback weight u_i is independently sampled from $\mathcal{N}(0, 1)$. In essence, δ is related to the readout error. For example, optimizing a mean-squared error between actual and target outputs, the readout weight dynamics will approach the steady state $w_i^* = -\frac{c\mu}{\lambda} \phi(x_i^\mu)$, where μ is the current

training example, ϵ_μ is the readout error, and λ is the weight-decay parameter. Hence, the last term in Eq. (5) captures the rank-one perturbation $\Delta\mathbf{J} = \mathbf{u}\mathbf{w}^\top$ [27].

The third plasticity is the well-known homeostatic plasticity. The homeostatic plasticity is an important partner of Hebbian one, discovered in cortical networks [30]. It commonly includes two types—multiplicative scaling of synaptic strength and activity-dependent stabilization of synaptic connections. Both types allow the network to satisfy the joint requirement of adaptation and stability. The latter one can be controlled by sleep and wake brain states [32] and was further explored to support stable self-sustained dynamics [31]. Hence, in this work, we consider the activity-dependent one, namely neuronal firing rate homeostasis:

$$J_{ij} = J_{ij}^0 - \frac{k}{N} [\phi(x_i) - r_{\text{tg}}] \phi(x_j), \quad (6)$$

where r_{tg} is the homeostatic setpoint of firing rates, and k indicates a learning rate. In all three plasticity rules, the rank-one modification at the single synapse level is negligible but produces a meaningful impact on the global behavior of the network [25] (see also our following replica calculations). Note also that the modification is asymmetric in the latter two forms of plasticity, in contrast to the Hebbian one which could slow or suppress the chaotic fluctuation.

Taking into account the aforementioned plasticity rules, we write the fixed-point distribution under learning as an optimization:

$$E_\ell(\mathbf{x}) = \frac{1}{2} \sum_i \left(-x_i + \sum_j [J_{ij}^0 + \Delta J_{ij}] \phi(x_j) \right)^2 + \eta \|\mathbf{x}\|^2, \quad (7)$$

where ΔJ_{ij} is the aforementioned activity-dependent modification to the random untrained part J_{ij}^0 . Therefore, the fixed-point state follows a Boltzmann distribution $P(\mathbf{x}) = \frac{1}{Z_\ell} e^{-\beta E_\ell(\mathbf{x})}$, where the learning related partition function Z_ℓ is a central quantity in this paper.

We finally remark that ΔJ_{ij} is the stationary solution of the following synaptic dynamics:

$$(1 + \tau \partial_t) \mathbf{L}(t) = \Delta \mathbf{J}(t), \quad (8)$$

where the synaptic time scale $\tau > 1$ (in a biological plausible sense that the plasticity dynamics is slower than the neural dynamics), the time-dependent plasticity $\mathbf{L}(t)$ is added to the random substrate \mathbf{J}^0 to form an intact \mathbf{J} , which further impacts the neural dynamics [Eq. (1)]. In simulations, we shall support our theoretical results with the numerical solutions of the above coupled dynamics.

C. Emergence of order from apparent disorder

Now, we clarify steps to observe an emergence of order from apparent disorder in the network coupling. For the canonical ensemble of learning, we must compute the free energy function $f \equiv -T \ln Z_\ell$, where we take the unit Boltzmann constant as commonly adopted in statistical mechanics of optimization problems [37], and clearly the partition function depends on the coupling realization. Hence, to obtain universal properties of the free energy, one has to calculate the disorder averaged free energy, which is tractable due to the following replica trick [38, 39]:

$$-\beta f = \frac{1}{N} \langle \ln Z_\ell(\mathbf{J}) \rangle_{\mathbf{J}} = \lim_{n \rightarrow 0} \frac{1}{nN} \ln \langle Z_\ell^n(\mathbf{J}) \rangle_{\mathbf{J}}, \quad (9)$$

which corresponds to taking the vanishing rate function in the large deviation principle [40]. The average over \mathbf{J} may also include the randomness of the feedback weights for the feedback learning. The replicated partition function reads,

$$\begin{aligned} Z_\ell^n(\mathbf{J}) &= \int d\mathbf{x} \exp \left[-\beta \left(\frac{1}{2} \sum_{i,a} \left(-x_i^a + \sum_j J_{ij} \phi(x_j^a) \right)^2 + \eta \sum_a \|\mathbf{x}^a\|^2 \right) \right], \\ &= \int d\mathbf{x} D\hat{\mathbf{x}} \exp \left[i\sqrt{\beta} \sum_{i,a} \hat{x}_i^a \left(-x_i^a + \sum_j J_{ij} \phi(x_j^a) \right) - \beta\eta \sum_a \|\mathbf{x}^a\|^2 \right], \end{aligned} \quad (10)$$

where $J_{ij} = J_{ij}^0 + \Delta J_{ij}$, $d\mathbf{x} \equiv \prod_{i=1}^N \prod_{a=1}^n dx_i^a$, $D\hat{\mathbf{x}} \equiv \prod_{i=1}^N \prod_{a=1}^n D\hat{x}_i^a$ where $D\hat{x} \equiv e^{-\frac{1}{2}\hat{x}^2} d\hat{x}/\sqrt{2\pi}$ is the Gaussian measure introduced during the linearization of the quadratic term through the Hubbard-Stratonovich transformation. We also introduce the replica index a which runs from 1 to n , and the subscript i represents the neuron index, which runs from 1 to N .

After performing the quenched disorder average $\langle \cdot \rangle_{\mathbf{J}}$ (details provided in Appendix A), we naturally introduce two physically meaningful order parameters:

$$\begin{aligned} Q^{ab} &= \frac{1}{N} \sum_i \phi(x_i^a) \phi(x_i^b), \\ R^a &= \frac{1}{N} \sum_i \hat{x}_i^a \phi(x_i^a). \end{aligned} \quad (11)$$

The first order parameter characterizes the fluctuation of the neural firing rates, a plausible quantity for detecting phase transitions, while the second order parameter corresponds to the response function in statistical physics, since it is in fact the derivative of the mean

population activity with respect to external perturbation of a small current [15]. In this sense, the abstract overlap matrix (\mathbf{Q} and \mathbf{R}) can be linked to the measurable neural activity in the complex dynamical system. At the first level of approximation, which can be cross-checked by experiments and the stability of the resultant mean-field equations, we write the following replica symmetric (RS) ansatz,

$$\begin{aligned} Q^{ab} &= q\delta_{ab} + Q(1 - \delta_{ab}), \\ R^a &= r. \end{aligned} \tag{12}$$

Under this RS ansatz, we derive the following free energy functions and associated single-variable effective Hamiltonians for three types of learning rules. Technical details are given in Appendix A.

Hebbian learning.—The free energy reads

$$-\beta f = \frac{1}{2}Q\hat{Q} - q\hat{q} - r\hat{r} - \ln \sigma + k\sqrt{\beta}rq + \ln \int DuDvI, \tag{13}$$

where $\sigma \equiv \sqrt{1 + g^2\beta(q - Q)}$, \hat{Q} , \hat{q} and \hat{r} are conjugated order parameters, and $I \equiv \int dx e^{\mathcal{H}(x)}$. The effective Hamiltonian of the Hebbian learning is given by

$$\mathcal{H}(x) \equiv -\beta\eta x^2 + \frac{1}{2}(2\hat{q} - \hat{Q})\phi^2(x) + \sqrt{\hat{Q}}u\phi(x) - \frac{1}{2\sigma^2}(g\sqrt{\beta Q}v + \hat{r}\phi(x) - \sqrt{\beta}x)^2. \tag{14}$$

Feedback learning.—The free energy reads

$$-\beta f = \frac{1}{2}Q\hat{Q} - q\hat{q} - \ln \sigma + \int DuDv \ln I, \tag{15}$$

where $I \equiv \int dx e^{\mathcal{H}(x)}$, and the corresponding effective Hamiltonian reads

$$\mathcal{H}(x) \equiv -\beta\eta x^2 + \frac{1}{2}(2\hat{q} - \hat{Q})\phi^2(x) + \sqrt{\hat{Q}}u\phi(x) - \frac{1}{2\sigma^2} \left(\sqrt{\beta g^2 Q + \beta \delta^2 q^2} v - \sqrt{\beta}x \right)^2. \tag{16}$$

Homeostatic learning.—The free energy reads

$$-\beta f = \frac{1}{2}Q\hat{Q} - q\hat{q} - r\hat{r} - \ln \sigma - k\sqrt{\beta}rq + \ln \int DuDvI, \tag{17}$$

where $I \equiv \int dx e^{\mathcal{H}(x)}$, and the corresponding effective Hamiltonian reads

$$\mathcal{H}(x) \equiv -\beta\eta x^2 + \frac{1}{2}(2\hat{q} - \hat{Q})\phi^2(x) + \sqrt{\hat{Q}}u\phi(x) - \frac{1}{2\sigma^2}(g\sqrt{\beta Q}v + \hat{r}\phi(x) - \sqrt{\beta}x + \sqrt{\beta}kr_{\text{tg}}q)^2. \tag{18}$$

Next, we send the temperature to zero for concentrating the Boltzmann measure on the ground state, i.e., zero-speed points in the phase space. In this limit, we have to properly

rescale the order parameters because of divergence behavior observed when $\beta \rightarrow \infty$. A reasonable scaling behavior is specified below.

$$\begin{aligned}
(q - Q) &\rightarrow \frac{\chi}{\beta}, \\
(2\hat{q} - \hat{Q}) &\rightarrow \beta\hat{\chi}, \\
\hat{q} &\rightarrow \beta^2\hat{q}, \\
r &\rightarrow \sqrt{\beta}r, \\
\hat{r} &\rightarrow \sqrt{\beta}\hat{r},
\end{aligned} \tag{19}$$

This allows us to obtain the zero-temperature free energy, and the corresponding saddle point equations in the thermodynamic limit. The saddle point equations are obtained by setting the derivative of the free energy with respect to the associated order parameters and their conjugate counterparts zero. Detailed analyses are given in Appendix A. Here, we summarize the main results.

Hebbian learning.—The free energy reads

$$-f = -\frac{1}{2}(q\hat{\chi} + 2\hat{q}\chi) - r\hat{r} + krq + \int DuDv\mathcal{H}_0(x^*), \tag{20}$$

where $x^* = \operatorname{argmax}_x \mathcal{H}_0(x)$, and

$$\mathcal{H}_0(x) = -\eta x^2 + \frac{1}{2}\hat{\chi}\phi^2(x) + \sqrt{2\hat{q}}u\phi(x) - \frac{1}{2\sigma^2}(g\sqrt{q}v + \hat{r}\phi(x) - x)^2, \tag{21}$$

with the following zero-temperature saddle-point equations (SDEs):

$$\begin{aligned}
q &= [\phi^2(x^*)], \\
\chi &= \frac{1}{\sqrt{2\hat{q}}} [u\phi(x^*)], \\
\hat{q} &= \frac{g^2}{2\sigma^4} (g^2q + \hat{r}^2 [\phi^2(x^*)] + [(x^*)^2] + 2g\sqrt{q}\hat{r} [v\phi(x^*)] - 2g\sqrt{q} [vx^*] - 2\hat{r} [x^*\phi(x^*)]), \\
\hat{\chi} &= 2kr - \frac{g^2}{\sigma^2} - \frac{g\hat{r}}{\sigma^2\sqrt{q}} [v\phi(x^*)] + \frac{g}{\sigma^2\sqrt{q}} [vx^*], \\
r &= -\frac{g\sqrt{q}}{\sigma^2} [v\phi(x^*)] - \frac{\hat{r}}{\sigma^2} [\phi^2(x^*)] + \frac{1}{\sigma^2} [x^*\phi(x^*)], \\
\hat{r} &= kq,
\end{aligned} \tag{22}$$

where $[\bullet] \equiv \int DuDv\bullet$ as before, and to estimate this average, we first generate M Monte Carlo samples $\{(u_i, v_i)\}_{i=1}^M$, for each of them we find the global maximum of $\mathcal{H}_0(x)$, i.e., x^* .

All these values corresponding to the maxima [for each pair of (u, v)] are further used to complete the calculation of the order parameter for one round of iteration.

Feedback learning.—The free energy reads

$$-f = -\frac{1}{2}(q\hat{\chi} + 2\hat{q}\chi) + \int (DuDv)\mathcal{H}_0(x^*), \quad (23)$$

where $x^* = \operatorname{argmax}_x \mathcal{H}_0(x)$, and

$$\mathcal{H}_0(x) = -\eta x^2 + \frac{1}{2}\hat{\chi}\phi^2(x) + \sqrt{2\hat{q}}u\phi(x) - \frac{1}{2\sigma^2}(\sqrt{g^2q + \delta^2q^2}v - x)^2, \quad (24)$$

with the following zero-temperature saddle point equations:

$$\begin{aligned} q &= [\phi^2(x^*)], \\ \chi &= \frac{1}{\sqrt{2\hat{q}}} [u\phi(x^*)], \\ \hat{q} &= \frac{g^2}{2\sigma^4} \left(g^2q + \delta^2q^2 + [(x^*)^2] - 2\sqrt{g^2q + \delta^2q^2} [vx^*] \right), \\ \hat{\chi} &= -\frac{g^2}{\sigma^2} - \frac{2q\delta^2}{\sigma^2} + \frac{g^2 + 2q\delta^2}{\sigma^2\sqrt{g^2q + \delta^2q^2}} [vx^*], \\ r &= -\frac{\sqrt{g^2q + \delta^2q^2}}{\sigma^2} [v\phi(x^*)] + \frac{1}{\sigma^2} [x^*\phi(x^*)], \end{aligned} \quad (25)$$

where we must remark that the response function in the last line is not a natural order parameter emerging from the disorder average, but can be computed from a moment generating function detailed in Appendix A.

Homeostatic learning.—The free energy reads

$$-f = -\frac{1}{2}(q\hat{\chi} + 2\hat{q}\chi) - r\hat{r} - krq + \int (DuDv)\mathcal{H}_0(x^*), \quad (26)$$

where $x^* = \operatorname{argmax}_x \mathcal{H}_0(x)$, and

$$\mathcal{H}_0(x) = -\eta x^2 + \frac{1}{2}\hat{\chi}\phi^2(x) + \sqrt{2\hat{q}}u\phi(x) - \frac{1}{2\sigma^2}(g\sqrt{q}v + \hat{r}\phi(x) - x + kr_{\text{tg}}q)^2, \quad (27)$$

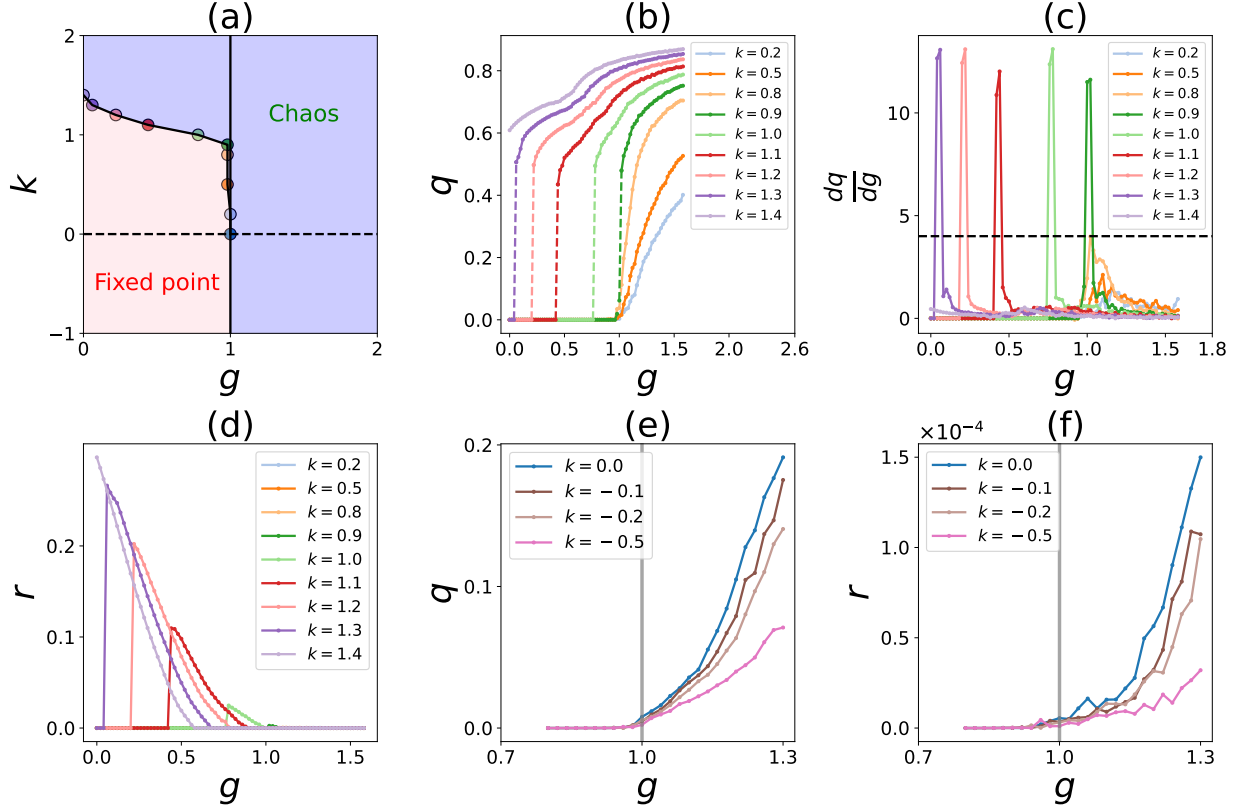


FIG. 1: Phase diagram and order parameters with varying g under Hebbian plasticity of different plasticity strengths. (a) The phase diagram is divided into two regions: the pink-colored area represents the fixed-point region, while the blue-colored area represents the chaotic region. (b,d) Plots of order parameters q and r against g for different positive values of k . In (c), the plot shows the derivative of q with respect to g . The dashed lines in (b) indicate the point where a first-order phase transition occurs, and in (c), the dashed line marks a sharp increase of the order parameter q . The threshold for the sharp slope is set to 4.0. (e-f) Plots of order parameters q and r against g for different negative values of k . The dashed line in (e) indicates the phase transition point. Results are the averages over five independent runs of the SDE solver (see Appendix B).

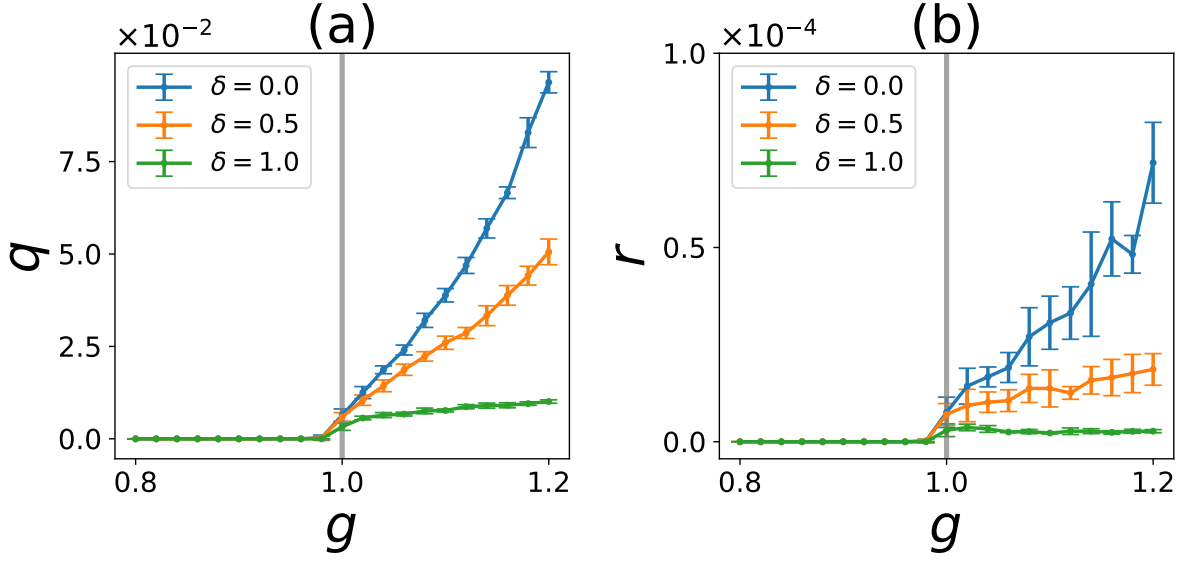


FIG. 2: The profile of the order parameters q and r with respect to the gain parameter g and the strength of feedback learning $\delta \in \{0.0, 0.5, 1.0\}$. The dashed line in (a) indicates the phase transition point. Five independent runs of the SDE solver are considered.

with the following zero-temperature SDEs:

$$\begin{aligned}
q &= [\phi^2(x^*)], \\
\chi &= \frac{1}{\sqrt{2\hat{q}}} [u\phi(x^*)], \\
\hat{q} &= \frac{g^2}{2\sigma^4} (g^2q + k^2r_{\text{tg}}^2q^2 + \hat{r}^2 [\phi^2(x^*)] + [(x^*)^2] + 2g\sqrt{q}\hat{r} [v\phi(x^*)] - 2g\sqrt{q} [vx^*] - 2\hat{r} [x^*\phi(x^*)] \\
&\quad + 2k\hat{r}r_{\text{tg}}q [\phi(x^*)] - 2kr_{\text{tg}}q [x^*]), \\
\hat{\chi} &= -2kr - \frac{g^2}{\sigma^2} - \frac{2k^2r_{\text{tg}}^2q}{\sigma^2} - \frac{g\hat{r}}{\sigma^2\sqrt{q}} [v\phi(x^*)] + \frac{g}{\sigma^2\sqrt{q}} [vx^*] - \frac{2}{\sigma^2}k\hat{r}r_{\text{tg}} [\phi(x^*)] + \frac{2}{\sigma^2}kr_{\text{tg}} [x^*], \\
r &= -\frac{g\sqrt{q}}{\sigma^2} [v\phi(x^*)] - \frac{\hat{r}}{\sigma^2} [\phi^2(x^*)] + \frac{1}{\sigma^2} [x^*\phi(x^*)] - \frac{kr_{\text{tg}}q}{\sigma^2} [\phi(x^*)], \\
\hat{r} &= -kq.
\end{aligned} \tag{28}$$

III. RESULTS AND DISCUSSION

For simplicity, we set $\eta = 0$ in the following discussion. We first show the theoretical results of Hebbian learning in Fig. 1. In the (k, g) plane, there appear two different dynamics

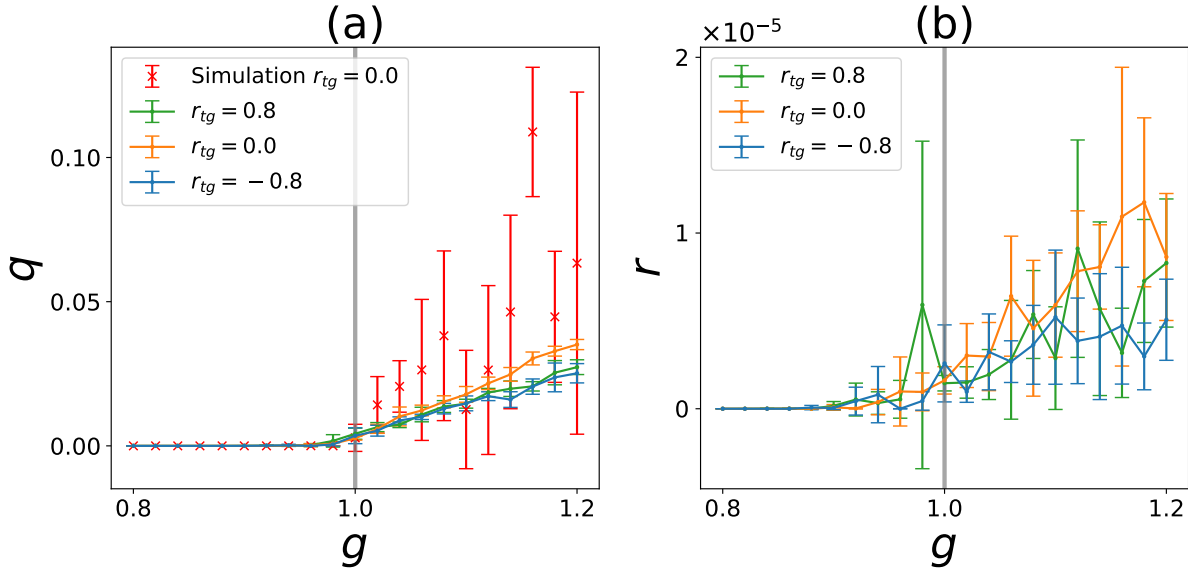


FIG. 3: The profile of the order parameters with respect to the gain parameter g and the target firing rate of homeostatic learning $r_{tg} \in \{-0.8, 0.0, 0.8\}$. The learning strength k is set to 0.5; we also present the simulation results for $r_{tg} = 0$ in networks of $N = 1000$ ($\tau = 0$). The simulation results are averages over the last 500 time steps. Five independent runs are used to obtain the averaged data points.

regimes. When $k < 0.8$, the chaos transition is continuous, while a larger value of k would trigger a discontinuous chaos transition, as supported by the q -profile and its derivatives [see Fig. 1 (b,c)]. In particular, a high value of k will shift the onset of a chaos transition to a smaller synaptic gain parameter (than a standard value of $g_c = 1$ for $k = 0$). Note that in our case, the original non-reciprocal coupling is directly added by the Hebbian term (equivalently, $\tau \rightarrow 0$ —a very fast dynamics). In this sense, our results are different from a recent study of finite τ using dynamical mean-field theory [25]. Moreover, our current analysis could not distinguish the internal refined structures of chaotic regimes. Perhaps, additional parameters need to be introduced. We leave this exciting extension to future works. The merit of our method lies in the clarification of dynamical phase transitions through well-defined order parameters optimizing a free energy function, rather than the activity auto-covariance in dynamical mean-field theory, where the transition to chaos is commonly determined by the change of the concavity of a classical potential [14].

In addition, our theory predicts that the response parameter displays a peak on the right-

hand side of the chaos transition point [Fig. 1 (d)]. The peak gets closer to the transition point once k becomes stronger. Moreover, the negative value of k does not alter the transition point and type [Fig. 1 (e,f)]. These properties reflect the nature of unstable fixed points of the out-of-equilibrium dynamics. If a finite speed (but still small in magnitude) of dynamics is considered, i.e., studying the finite temperature case, one would obtain a peak at the exact onset of the chaos, as already shown in the non-plastic model [15].

We next look at the theory of feedback learning (Fig. 2). Our theory predicts that tuning the feedback strength does not change the type of dynamics transition and the transition location. However, stronger feedback would limit the dynamics diversity, as expected from the readout error nature of the feedback strength.

We finally study the firing rate homeostatic learning. Given the plasticity strength k , we do not observe a qualitative change of the chaos transition (including the onset point) when varying different target rates (Fig. 3). In fact, by setting $r_{\text{tg}} = 0$, we recover the Hebbian learning case with negative strength (or anti-Hebbian plasticity). However, increasing further the target rate will make the network enter the non-trivial-fixed-point phase. We thus conclude that the homeostatic learning does not shift the chaos transition compared to the corresponding non-plastic counterpart, while the activity magnitude can be suppressed by tuning the setpoint. Note that in Fig. 3 (a) there exists a gap between the theoretically-predicted unstable-fixed-points activity and the simulations (non-zero speed), as also proved in a recent work [18]. Figure 4 summarizes the representative dynamics trajectories when different plasticity rules are considered.

IV. CONCLUDING REMARKS

Coupled dynamics between neurons and synapses are ubiquitous in the brain. How to understand the nature of neuron-synapse interaction remains challenging in both theory and experiments. Here, we apply the quasi-potential method developed recently in analyzing non-plastic recurrent networks to address how learning induces dynamical transition in recurrent neural networks. Three types of plasticity rules are considered: Hebbian, feedback, and homeostatic plasticities. For simplification, we do not take into account the intrinsic time scales of synaptic dynamics, but instead, we focus on the fixed-point structure of the dynamics phase space. Our theoretical calculation reveals that in Hebbian learning, the

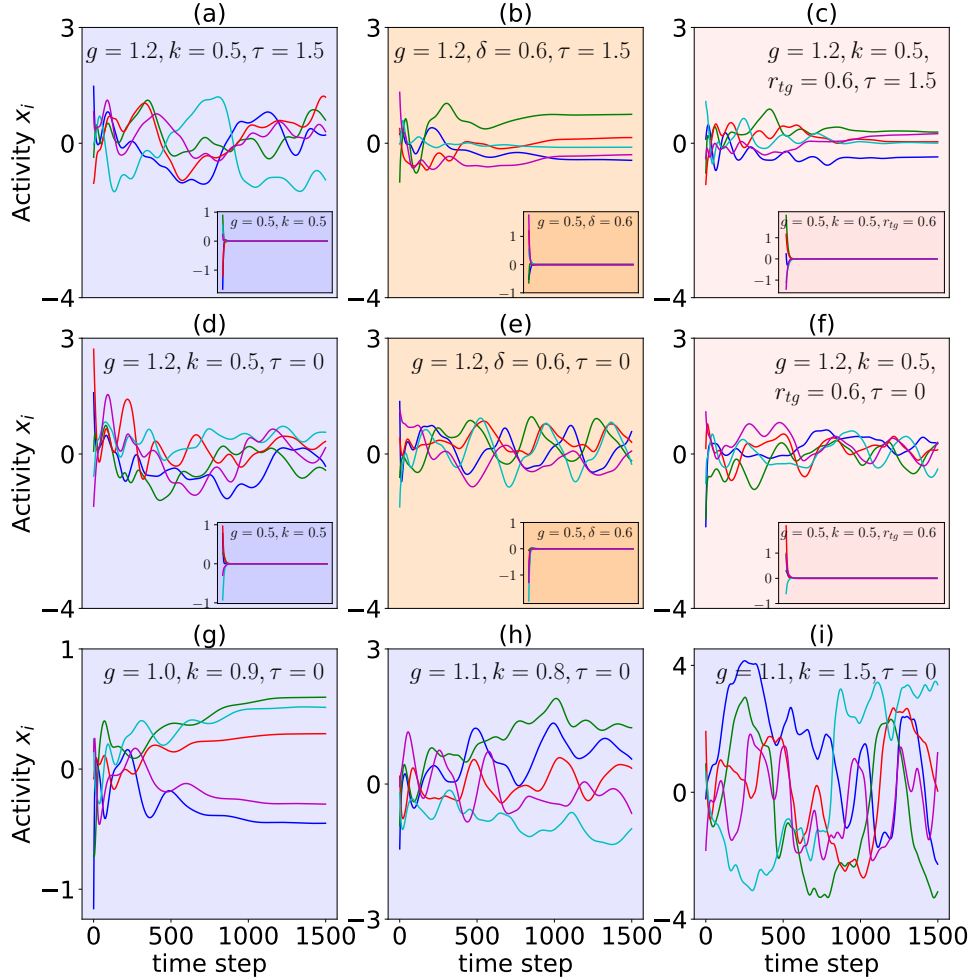


FIG. 4: Neural dynamics under different plasticity rules (a network of 1000 neurons, five of which are randomly selected and shown). Three different background colors distinguish different learning types. (a, d, g, h, i) Neural dynamics under Hebbian learning. In (a), the time constant $\tau = 1.5$; in (d, g, h, i), $\tau = 0$. In the main plot, parameters are $(g, k) = (1.2, 0.5)$, and in the inset plot parameters are $(g, k) = (0.5, 0.5)$. (b, e) Neural dynamics under feedback learning. In (b), $\tau = 1.5$; in (e), $\tau = 0$. In the main plot, parameters are $(g, \delta) = (1.2, 0.6)$, and in the inset parameters are $(g, \delta) = (0.5, 0.6)$. (c, f) Neural dynamics under homeostatic learning. In (c), $\tau = 1.5$; in (f), $\tau = 0$. In the main plot, parameters are $(g, k) = (1.2, 0.5)$, and $r_{tg} = 0.6$, and in the inset parameters are $(g, k) = (0.5, 0.5)$, and $r_{tg} = 0.6$.

Hebbian strength will alter the nature of the chaos transition. More precisely, when the strength grows above some threshold, a discontinuous chaos transition occurs at a smaller synaptic gain compared to the non-plastic network. Decreasing the Hebbian strength, a continuous chaos transition will be recovered. The dynamics simulation supports this theoretical finding. However, the feedback and homeostatic learning do not alter the location and type of the chaos transition. Only the chaotic fluctuation is tuned by the feedback strength, while a large target setpoint suppresses the chaotic fluctuation in the case of homeostatic learning.

In future works, it would be interesting to study the coupled dynamics by tuning separate inverse temperatures and monitoring the competition between neural and synaptic dynamics. It is also promising to investigate the impact of the change of chaos transition in improving generalization performances in recurrent computation [41–43], and even verify our theoretical predictions in neurobiological experiments. The study of coupled dynamics systems may also yield insights into neurological and psychiatric disorders.

Acknowledgments

This research was supported by the National Natural Science Foundation of China for Grant numbers 12475045 and 12122515, and Guangdong Provincial Key Laboratory of Magnetoelectric Physics and Devices (No. 2022B1212010008), and Guangdong Basic and Applied Basic Research Foundation (Grant No. 2023B1515040023).

Appendix A: Replica analysis details of non-equilibrium learning dynamics

1. Hebbian learning

Starting from the replicated partition function in the main text, we perform the disorder average as follows,

$$\begin{aligned}
\langle Z_\ell^n \rangle &= \left\langle \int d\mathbf{x} \exp \left[-\beta \left(\frac{1}{2} \sum_{ia} \left(-x_i^a + \sum_j J_{ij} \phi(x_j^a) \right)^2 + \eta \sum_a \|\mathbf{x}^a\|^2 \right) \right] \right\rangle \\
&= \left\langle \int d\mathbf{x} D\hat{\mathbf{x}} \exp \left[i\sqrt{\beta} \sum_{ia} \hat{x}_i^a \left(-x_i^a + \sum_j J_{ij} \phi(x_j^a) \right) - \beta\eta \sum_a \|\mathbf{x}^a\|^2 \right] \right\rangle.
\end{aligned} \tag{A1}$$

Due to the i.i.d. nature of the coupling statistics, the disorder average is straightforward.

$$\begin{aligned}
& \left\langle \exp \left[i\sqrt{\beta} \sum_{ij} J_{ij} \sum_a \hat{x}_i^a \phi(x_j^a) \right] \right\rangle \\
&= \left\langle \exp \left[i\sqrt{\beta} \sum_{ij} J_{ij}^0 \sum_a \hat{x}_i^a \phi(x_j^a) \right] \right\rangle \exp \left[i\frac{k\sqrt{\beta}}{N} \sum_{ij} \sum_a \hat{x}_i^a \phi(x_i^a) \phi^2(x_j^a) \right] \\
&= \exp \left[-\frac{1}{2} \frac{\beta g^2}{N} \sum_{ij} \left(\sum_a \hat{x}_i^a \phi(x_j^a) \right)^2 + i\frac{k\sqrt{\beta}}{N} \sum_{ij} \sum_a \hat{x}_i^a \phi(x_i^a) \phi^2(x_j^a) \right] \quad (\text{A2}) \\
&= \exp \left[-\frac{1}{2} \frac{\beta g^2}{N} \sum_{ij} \sum_{ab} \hat{x}_i^a \hat{x}_i^b \phi(x_j^a) \phi(x_j^b) + i\frac{k\sqrt{\beta}}{N} \sum_{ij} \sum_a \hat{x}_i^a \phi(x_i^a) \phi^2(x_j^a) \right] \\
&= \exp \left[-\frac{1}{2} \beta g^2 \sum_i \sum_{ab} \hat{x}_i^a \hat{x}_i^b Q^{ab} + ik\sqrt{\beta} N \sum_a R^a Q^{aa} \right],
\end{aligned}$$

where we have defined two kinds of order parameters:

$$\begin{aligned}
Q^{ab} &= \frac{1}{N} \sum_i \phi(x_i^a) \phi(x_i^b), \\
R^a &= \frac{1}{N} \sum_i \hat{x}_i^a \phi(x_i^a).
\end{aligned} \quad (\text{A3})$$

Inserting the following identity into Eq. (A1), we can further simplify the above result.

$$\begin{aligned}
1 &= \prod_{a \leq b} \int dQ^{ab} \delta \left(Q^{ab} - \frac{1}{N} \sum_i \phi(x_i^a) \phi(x_i^b) \right) \prod_a \int dR^a \delta \left(R^a - \frac{1}{N} \sum_i \hat{x}_i^a \phi(x_i^a) \right) \\
&= \int \frac{d\mathbf{Q} d\hat{\mathbf{Q}} d\mathbf{R} d\hat{\mathbf{R}}}{2\pi} \exp \left[-i \sum_{a \leq b} Q^{ab} \hat{Q}^{ab} - i \sum_a R^a \hat{R}^a + i \frac{1}{N} \sum_i \sum_{a \leq b} \hat{Q}^{ab} \phi(x_i^a) \phi(x_i^b) \right. \\
&\quad \left. + i \frac{1}{N} \sum_a \hat{R}^a \sum_i \hat{x}_i^a \phi(x_i^a) \right] \quad (\text{A4}) \\
&= \int \frac{d\mathbf{Q} d\hat{\mathbf{Q}} d\mathbf{R} d\hat{\mathbf{R}}}{2\pi i/N} \exp \left[-N \sum_{a \leq b} Q^{ab} \hat{Q}^{ab} - N \sum_a R^a \hat{R}^a + \sum_i \sum_{a \leq b} \hat{Q}^{ab} \phi(x_i^a) \phi(x_i^b) \right. \\
&\quad \left. + i \sum_a \hat{R}^a \sum_i \hat{x}_i^a \phi(x_i^a) \right],
\end{aligned}$$

where we have rescaled the order parameters as $\hat{Q}^{ab} \rightarrow -iN\hat{Q}^{ab}$, $R^a \rightarrow -iR^a$ and $\hat{R}^a \rightarrow N\hat{R}^a$.

Therefore, the averaged replicated partition function becomes

$$\begin{aligned}
\langle Z_\ell^n \rangle &\propto \int d\mathbf{x} D\hat{\mathbf{x}} d\mathbf{Q} d\hat{\mathbf{Q}} d\mathbf{R} d\hat{\mathbf{R}} \exp \left[-i\sqrt{\beta} \sum_{ia} x_i^a \hat{x}_i^a - \beta\eta \sum_{ia} (x_i^a)^2 - \frac{1}{2}g^2\beta \sum_{ab} Q^{ab} \left(\sum_i \hat{x}_i^a \hat{x}_i^b \right) \right. \\
&\quad \left. + k\sqrt{\beta}N \sum_a R^a Q^{aa} - N \sum_{a \leq b} Q^{ab} \hat{Q}^{ab} - N \sum_a R^a \hat{R}^a + \sum_i \sum_{a \leq b} \hat{Q}^{ab} \phi(x_i^a) \phi(x_i^b) \right. \\
&\quad \left. + i \sum_a \hat{R}^a \sum_i \hat{x}_i^a \phi(x_i^a) \right] \\
&= \int d\mathbf{Q} d\hat{\mathbf{Q}} d\mathbf{R} d\hat{\mathbf{R}} \exp \left[N \left(- \sum_{a \leq b} Q^{ab} \hat{Q}^{ab} - \sum_a R^a \hat{R}^a + G \right) \right],
\end{aligned} \tag{A5}$$

where \propto means that we have neglected irrelevant pre-factors, and the auxiliary quantity

$$\begin{aligned}
G &= \ln \int d\mathbf{x} D\hat{\mathbf{x}} \exp \left[-i\sqrt{\beta} \sum_a x^a \hat{x}^a - \beta\eta \sum_a (x^a)^2 - \frac{1}{2}g^2\beta \sum_{ab} Q^{ab} \hat{x}^a \hat{x}^b + \sum_{a \leq b} \hat{Q}^{ab} \phi(x^a) \phi(x^b) \right. \\
&\quad \left. + k\sqrt{\beta} \sum_a R^a Q^{aa} + i \sum_a \hat{R}^a \hat{x}^a \phi(x^a) \right].
\end{aligned} \tag{A6}$$

To proceed, we have to adopt the RS ansatz:

$$\begin{aligned}
Q^{ab} &= q\delta_{ab} + Q(1 - \delta_{ab}), \\
R^a &= r.
\end{aligned} \tag{A7}$$

It then follows that

$$\begin{aligned}
& - \frac{1}{2}g^2\beta \sum_{ab} Q^{ab} \hat{x}^a \hat{x}^b + \sum_{a \leq b} \hat{Q}^{ab} \phi(x^a) \phi(x^b) \\
&= - \frac{1}{2}g^2\beta \left(Q \left(\sum_a \hat{x}^a \right)^2 + (q - Q) \sum_a (\hat{x}^a)^2 \right) + \frac{1}{2}\hat{Q} \left(\sum_a \phi(x^a) \right)^2 + \left(\hat{q} - \frac{1}{2}\hat{Q} \right) \left(\sum_a \phi^2(x^a) \right).
\end{aligned} \tag{A8}$$

We can then observe that the n -dimensional integral in Eq. (A6) factorizes over the replica index.

After completing the following integral over \hat{x} :

$$\begin{aligned}
& \int D\hat{x} \exp \left[-\frac{1}{2}g^2\beta(q - Q)\hat{x}^2 + i(g\sqrt{\beta Q}v + \hat{r}\phi(x) - \sqrt{\beta x})\hat{x} \right] \\
&= \frac{1}{\sigma} \exp \left[-\frac{1}{2} \frac{1}{\sigma^2} (g\sqrt{\beta Q}v + \hat{r}\phi(x) - \sqrt{\beta x})^2 \right],
\end{aligned} \tag{A9}$$

where $\sigma \equiv \sqrt{1 + g^2\beta(q - Q)}$, we arrive at the following neat formula:

$$G = -n \ln \sigma + k\sqrt{\beta}nrq + \ln \int DuDvI^n, \quad (\text{A10})$$

where $I \equiv \int dx e^{\mathcal{H}(x)}$ and the effective single-variable Hamiltonian can be read off,

$$\mathcal{H}(x) \equiv -\beta\eta x^2 + \frac{1}{2}(2\hat{q} - \hat{Q})\phi^2(x) + \sqrt{\hat{Q}}u\phi(x) - \frac{1}{2\sigma^2}(g\sqrt{\beta Q}v + \hat{r}\phi(x) - \sqrt{\beta}x)^2. \quad (\text{A11})$$

Following the replica trick, the free energy in the finite temperature is given by

$$-\beta f = \frac{1}{2}Q\hat{Q} - q\hat{q} - r\hat{r} - \ln \sigma + k\sqrt{\beta}rq + \ln \int DuDvI. \quad (\text{A12})$$

However, we are interested in the zero temperature limit, which makes us see the fixed points of the non-gradient out-of-equilibrium dynamics. Under the scaling behavior of the order parameters in the main text, one can derive that

$$\begin{aligned} Q &= q - (q - Q) \Rightarrow Q = q - \frac{1}{\beta}\chi \rightarrow q, \\ \hat{Q} &= 2\hat{q} - (2\hat{q} - \hat{Q}) \Rightarrow \hat{Q} = 2\beta^2\hat{q} - \beta\hat{\chi} \rightarrow 2\beta^2\hat{q}. \end{aligned} \quad (\text{A13})$$

Hence, the effective Hamiltonian $\mathcal{H}(x)$ behaves as an explicit linear function of β , written as follows.

$$\begin{aligned} \mathcal{H}(x) &\equiv -\beta\eta x^2 + \frac{1}{2}(2\hat{q} - \hat{Q})\phi^2(x) + \sqrt{\hat{Q}}u\phi(x) - \frac{1}{2\sigma^2}(g\sqrt{\beta Q}v + \hat{r}\phi(x) - \sqrt{\beta}x)^2 \\ &\Rightarrow -\beta\eta x^2 + \frac{1}{2}\beta\hat{\chi}\phi^2(x) + \beta\sqrt{2\hat{q}}u\phi(x) - \frac{\beta}{2\sigma^2}(g\sqrt{q}v + \hat{r}\phi(x) - x)^2 \equiv \beta\mathcal{H}_0(x). \end{aligned} \quad (\text{A14})$$

Here $\sigma = \sqrt{1 + \beta g^2(q - Q)} \rightarrow \sqrt{1 + g^2\chi}$ is a quantity of $\mathcal{O}(1)$. This result further implies that,

$$\begin{aligned} -\beta f &= \frac{1}{2}Q\hat{Q} - q\hat{q} - r\hat{r} - \ln \sigma + k\sqrt{\beta}rq + \int DuDv \ln \int dx e^{\mathcal{H}(x)} \\ &= -\frac{1}{2} \left[q(2\hat{q} - \hat{Q}) + \hat{Q}(q - Q) \right] - r\hat{r} - \ln \sigma + k\sqrt{\beta}rq + \int DuDv \ln \int dx e^{\mathcal{H}(x)}, \\ &\Rightarrow -\beta f \rightarrow -\frac{1}{2}\beta(q\hat{\chi} + 2\hat{q}\chi) - \beta r\hat{r} - \ln \sigma + \beta krq + \int DuDv \ln \int dx e^{\beta\mathcal{H}_0(x)}. \end{aligned} \quad (\text{A15})$$

We can then conclude that the free energy in the zero temperature must take the following form:

$$-f = -\frac{1}{2}(q\hat{\chi} + 2\hat{q}\chi) - r\hat{r} + krq + \int DuDv \mathcal{H}_0(x^*), \quad (\text{A16})$$

where $x^* = \operatorname{argmax}_x \mathcal{H}_0(x)$. $\mathcal{H}_0(x)$ has been derived in Eq. (A14).

$$\mathcal{H}_0(x) = -\eta x^2 + \frac{1}{2} \hat{\chi} \phi^2(x) + \sqrt{2\hat{q}} u \phi(x) - \frac{1}{2\sigma^2} (g\sqrt{q}v + \hat{r}\phi(x) - x)^2. \quad (\text{A17})$$

Optimization of $\mathcal{H}_0(x)$ is a direct consequence of applying Laplace method to obtain the last integral in Eq. (A16).

Finally, we can set the derivative of the zero-temperature free energy with respect to all relevant order parameters zero, from which the SDEs can be derived as follows.

$$\begin{aligned} q &= [\phi^2(x^*)], \\ \chi &= \frac{1}{\sqrt{2\hat{q}}} [u\phi(x^*)], \\ \hat{q} &= \frac{g^2}{2\sigma^4} (g^2q + \hat{r}^2 [\phi^2(x^*)] + [(x^*)^2] + 2g\sqrt{q}\hat{r} [v\phi(x^*)] - 2g\sqrt{q} [vx^*] - 2\hat{r} [x^*\phi(x^*)]), \\ \hat{\chi} &= 2kr - \frac{g^2}{\sigma^2} - \frac{g\hat{r}}{\sigma^2\sqrt{q}} [v\phi(x^*)] + \frac{g}{\sigma^2\sqrt{q}} [vx^*], \\ r &= -\frac{g\sqrt{q}}{\sigma^2} [v\phi(x^*)] - \frac{\hat{r}}{\sigma^2} [\phi^2(x^*)] + \frac{1}{\sigma^2} [x^*\phi(x^*)], \\ \hat{r} &= kq, \end{aligned} \quad (\text{A18})$$

where $[\bullet] \equiv \int DuDv\bullet$ as before, and to estimate this average, we first generate M Monte Carlo samples $\{(u_i, v_i)\}_{i=1}^M$, for each of them we find the global maximum of $\mathcal{H}_0(x)$, i.e., x^* . All these values corresponding to the maxima [for each pair of (u, v)] are further used to complete the calculation of the order parameter for one round of iteration.

2. Feedback learning

We next turn to the feedback learning. Note that in the feedback learning, we have an extra randomness from the feedback weight \mathbf{u} . The disorder average part is thus calculated

as follows.

$$\begin{aligned}
& \left\langle \exp \left[i\sqrt{\beta} \sum_{ij} J_{ij} \sum_a \hat{x}_i^a \phi(x_j^a) \right] \right\rangle \\
&= \left\langle \exp \left[i\sqrt{\beta} \sum_{ij} J_{ij}^0 \sum_a \hat{x}_i^a \phi(x_j^a) \right] \right\rangle_{\mathbf{J}^0} \left\langle \exp \left[i\frac{\sqrt{\beta}}{N} \delta \sum_{ij} u_i \sum_a \hat{x}_i^a \phi^2(x_j^a) \right] \right\rangle_{\mathbf{u}} \\
&= \exp \left[-\frac{1}{2} \frac{\beta g^2}{N} \sum_{ij} \left(\sum_a \hat{x}_i^a \phi(x_j^a) \right)^2 - \frac{1}{2} \frac{\beta}{N^2} \delta^2 \sum_i \left(\sum_j \sum_a \hat{x}_i^a \phi^2(x_j^a) \right)^2 \right] \quad (\text{A19}) \\
&= \exp \left[-\frac{1}{2} \frac{\beta g^2}{N} \sum_{ij} \sum_{ab} \hat{x}_i^a \hat{x}_i^b \phi(x_j^a) \phi(x_j^b) - \frac{1}{2} \frac{\beta}{N^2} \delta^2 \sum_{ijk} \sum_{ab} \hat{x}_i^a \hat{x}_i^b \phi^2(x_j^a) \phi^2(x_k^b) \right] \\
&= \exp \left[-\frac{1}{2} \beta g^2 \sum_i \sum_{ab} \hat{x}_i^a \hat{x}_i^b Q^{ab} - \frac{1}{2} \beta \delta^2 \sum_i \sum_{ab} \hat{x}_i^a \hat{x}_i^b Q^{aa} Q^{bb} \right],
\end{aligned}$$

where the replica overlap matrix $Q^{ab} = \frac{1}{N} \sum_i \phi(x_i^a) \phi(x_i^b)$, has to be introduced through an integral of Dirac delta functions:

$$\begin{aligned}
1 &= \prod_{a \leq b} \int dQ^{ab} \delta \left(Q^{ab} - \frac{1}{N} \sum_i \phi(x_i^a) \phi(x_i^b) \right) \\
&= \int \frac{d\mathbf{Q} d\hat{\mathbf{Q}}}{2\pi} \exp \left[-i \sum_{a \leq b} Q^{ab} \hat{Q}^{ab} + i \frac{1}{N} \sum_i \sum_{a \leq b} \hat{Q}^{ab} \phi(x_i^a) \phi(x_i^b) \right] \quad (\text{A20}) \\
&= \int \frac{d\mathbf{Q} d\hat{\mathbf{Q}}}{2\pi i/N} \exp \left[-N \sum_{a \leq b} Q^{ab} \hat{Q}^{ab} + \sum_i \sum_{a \leq b} \hat{Q}^{ab} \phi(x_i^a) \phi(x_i^b) \right].
\end{aligned}$$

The n -th moment of the partition function can then be written as

$$\begin{aligned}
\langle Z_\ell^n \rangle &\propto \int d\mathbf{x} D\hat{\mathbf{x}} d\mathbf{Q} d\hat{\mathbf{Q}} \exp \left[-i\sqrt{\beta} \sum_{ia} x_i^a \hat{x}_i^a - \beta\eta \sum_{ia} (x_i^a)^2 - \frac{1}{2} g^2 \beta \sum_{ab} Q^{ab} \left(\sum_i \hat{x}_i^a \hat{x}_i^b \right) \right. \\
&\quad \left. - \frac{1}{2} \beta \delta^2 \sum_{ab} Q^{aa} Q^{bb} \left(\sum_i \hat{x}_i^a \hat{x}_i^b \right) - N \sum_{a \leq b} Q^{ab} \hat{Q}^{ab} + \sum_i \sum_{a \leq b} \hat{Q}^{ab} \phi(x_i^a) \phi(x_i^b) \right] \\
&\propto \int d\mathbf{Q} d\hat{\mathbf{Q}} \exp \left[N \left(- \sum_{a \leq b} Q^{ab} \hat{Q}^{ab} + G \right) \right], \quad (\text{A21})
\end{aligned}$$

where the model-dependent action reads

$$\begin{aligned}
G &= \ln \int d\mathbf{x} D\hat{\mathbf{x}} \exp \left[-i\sqrt{\beta} \sum_a x^a \hat{x}^a - \beta\eta \sum_a (x^a)^2 - \frac{1}{2} g^2 \beta \sum_{ab} Q^{ab} \hat{x}^a \hat{x}^b + \sum_{a \leq b} \hat{Q}^{ab} \phi(x^a) \phi(x^b) \right. \\
&\quad \left. - \frac{1}{2} \beta \delta^2 \sum_{ab} Q^{aa} Q^{bb} (\hat{x}^a \hat{x}^b) \right]. \quad (\text{A22})
\end{aligned}$$

We then adopt the RS ansatz once again. $Q^{ab} = q\delta_{ab} + Q(1 - \delta_{ab})$. The averaged replicated partition function yields a neat form:

$$\langle Z_\ell^n \rangle \propto \int (dQd\hat{Q}dqd\hat{q}) \exp \left[-N \left(\frac{n(n-1)}{2} Q\hat{Q} + nq\hat{q} \right) \right] \exp[NG], \quad (\text{A23})$$

where G is defined below:

$$\begin{aligned} G = \ln \int d\mathbf{x} D\hat{\mathbf{x}} \exp & \left[-i\sqrt{\beta} \sum_a x^a \hat{x}^a - \beta\eta \sum_a (x^a)^2 - \frac{1}{2}g^2\beta \left(Q \left(\sum_a \hat{x}^a \right)^2 + (q-Q) \sum_a (\hat{x}^a)^2 \right) \right. \\ & \left. + \frac{1}{2} \left(\hat{Q} \left(\sum_a \phi(x^a) \right)^2 + (2\hat{q} - \hat{Q}) \sum_a \phi^2(x^a) \right) - \frac{1}{2}\beta\delta^2q^2 \left(\sum_a \hat{x}^a \right)^2 \right]. \end{aligned} \quad (\text{A24})$$

Notice that G can be further simplified by linearizing the quadratic terms, i.e., by reversely applying a Gaussian integral identity $\int Dte^{bt} = e^{b^2/2}$. We then arrive at the following result:

$$\begin{aligned} G = \ln \int d\mathbf{x} D\hat{\mathbf{x}} (DuDv) \exp & \left[-i\sqrt{\beta} \sum_a x^a \hat{x}^a - \beta\eta \sum_a (x^a)^2 - \frac{1}{2}g^2\beta(q-Q) \sum_a (\hat{x}^a)^2 \right. \\ & \left. + \frac{1}{2}(2\hat{q} - \hat{Q}) \sum_a \phi^2(x^a) + i\sqrt{\beta g^2 Q + \beta\delta^2 q^2} v \sum_a \hat{x}^a + \sqrt{\hat{Q}u} \sum_a \phi(x^a) \right] \\ = \ln \int (DuDv) (I_1)^n, \end{aligned} \quad (\text{A25})$$

where the shorthand for the one-dimensional integral I_1 reads,

$$\begin{aligned} I_1 = \int (dx D\hat{x}) \exp & \left[-i\sqrt{\beta}x\hat{x} - \beta\eta x^2 - \frac{1}{2}g^2\beta(q-Q)\hat{x}^2 + \frac{1}{2}(2\hat{q} - \hat{Q})\phi^2(x) \right. \\ & \left. + i\sqrt{\beta g^2 Q + \beta\delta^2 q^2} v\hat{x} + \sqrt{\hat{Q}u}\phi(x) \right] \\ = \int dx \exp & \left[-\beta\eta x^2 + \frac{1}{2}(2\hat{q} - \hat{Q})\phi^2(x) + \sqrt{\hat{Q}u}\phi(x) \right] \int D\hat{x} \exp \left[-i\sqrt{\beta}x\hat{x} \right. \\ & \left. - \frac{1}{2}g^2\beta(q-Q)\hat{x}^2 + i\sqrt{\beta g^2 Q + \beta\delta^2 q^2} v\hat{x} \right] \\ = \int dx \frac{1}{\sigma} \exp & \left[-\beta\eta x^2 + \frac{1}{2}(2\hat{q} - \hat{Q})\phi^2(x) + \sqrt{\hat{Q}u}\phi(x) - \frac{1}{2\sigma^2} \left(\sqrt{\beta g^2 Q + \beta\delta^2 q^2} v - \sqrt{\beta}x \right)^2 \right], \end{aligned} \quad (\text{A26})$$

where $\sigma \equiv \sqrt{1 + g^2\beta(q-Q)}$.

The G function can be finally written in a neat form as follows:

$$G = -n \ln \sigma + \ln \int DuDv I^n, \quad (\text{A27a})$$

$$I \equiv \int dx e^{\mathcal{H}(x)}, \quad (\text{A27b})$$

where the single-variable effective Hamiltonian for the feedback learning is given below.

$$\mathcal{H}(x) \equiv -\beta\eta x^2 + \frac{1}{2}(2\hat{q} - \hat{Q})\phi^2(x) + \sqrt{\hat{Q}}u\phi(x) - \frac{1}{2\sigma^2} \left(\sqrt{\beta g^2 Q + \beta \delta^2 q^2 v} - \sqrt{\beta x} \right)^2. \quad (\text{A28})$$

Hence, applying the replica trick, we manage to complete the quenched disorder average and get the free energy.

$$-\beta f = \frac{1}{2}Q\hat{Q} - q\hat{q} - \ln \sigma + \int DuDv \ln I. \quad (\text{A29})$$

We are interested in the zero temperature limit with the same reason claimed before. To get a physically meaningful free energy in this limit, we have to adopt the following scaling behavior.

$$\begin{aligned} (q - Q) &\rightarrow \frac{\chi}{\beta}, \\ (2\hat{q} - \hat{Q}) &\rightarrow \beta\hat{\chi}, \\ q &\rightarrow q, \\ \hat{q} &\rightarrow \beta^2\hat{q}. \end{aligned} \quad (\text{A30})$$

One can thus get the scaling behavior of the effective Hamiltonian as follows,

$$\begin{aligned} \mathcal{H}(x) &\equiv -\beta\eta x^2 + \frac{1}{2}(2\hat{q} - \hat{Q})\phi^2(x) + \sqrt{\hat{Q}}u\phi(x) - \frac{1}{2\sigma^2}(\sqrt{\beta g^2 Q + \beta \delta^2 q^2 v} - \sqrt{\beta x})^2, \\ &\Rightarrow -\beta\eta x^2 + \frac{1}{2}\beta\hat{\chi}\phi^2(x) + \beta\sqrt{2\hat{q}}u\phi(x) - \frac{\beta}{2\sigma^2}(\sqrt{g^2 q + \delta^2 q^2 v} - x)^2 \equiv \beta\mathcal{H}_0(x), \end{aligned} \quad (\text{A31})$$

Here $\sigma = \sqrt{1 + \beta g^2(q - Q)} \rightarrow \sqrt{1 + g^2\chi}$.

The free energy can be derived by following the similar steps.

$$\begin{aligned} -\beta f &= \frac{1}{2}Q\hat{Q} - q\hat{q} - \ln \sigma + \int DuDv \ln \int dx e^{\mathcal{H}(x)} \\ &= -\frac{1}{2} \left[q(2\hat{q} - \hat{Q}) + \hat{Q}(q - Q) \right] - \ln \sigma + \int DuDv \ln \int dx e^{\mathcal{H}(x)} \\ &\Rightarrow -\frac{1}{2}\beta(q\hat{\chi} + 2\hat{q}\chi) - \ln \sigma + \int DuDv \ln \int dx e^{\beta\mathcal{H}_0(x)}, \end{aligned} \quad (\text{A32})$$

which gives rise to the zero-temperature free energy as follows.

$$-f = -\frac{1}{2}(q\hat{\chi} + 2\hat{q}\chi) + \int (DuDv) \mathcal{H}_0(x^*), \quad (\text{A33})$$

where $x^* = \operatorname{argmax}_x \mathcal{H}_0(x)$, and

$$\mathcal{H}_0(x) = -\eta x^2 + \frac{1}{2} \hat{\chi} \phi^2(x) + \sqrt{2\hat{q}} u \phi(x) - \frac{1}{2\sigma^2} (\sqrt{g^2 q + \delta^2 q^2} v - x)^2, \quad (\text{A34})$$

From the vanishing gradients of the free energy with respect to associated order parameters, we get the SDEs below:

$$\begin{aligned} q &= [\phi^2(x^*)], \\ \chi &= \frac{1}{\sqrt{2\hat{q}}} [u\phi(x^*)], \\ \hat{q} &= \frac{g^2}{2\sigma^4} \left(g^2 q + \delta^2 q^2 + [(x^*)^2] - 2\sqrt{g^2 q + \delta^2 q^2} [vx^*] \right), \\ \hat{\chi} &= -\frac{g^2}{\sigma^2} - \frac{2q\delta^2}{\sigma^2} + \frac{g^2 + 2q\delta^2}{\sigma^2 \sqrt{g^2 q + \delta^2 q^2}} [vx^*]. \end{aligned} \quad (\text{A35})$$

Because in the feedback learning, the response function can not be retrieved from the vanilla replica calculation, we can use the moment generating function to derive the response function. We thus modify the quasi-potential as

$$E_\ell(\mathbf{x}) = \frac{1}{2} \sum_i \left(-x_i + \sum_j J_{ij} \phi(x_j) + h_i \right)^2 + \eta \sum_i x_i^2 + \gamma \sum_i \phi(x_i), \quad (\text{A36})$$

where γ is a Lagrange parameter for the population current, and \mathbf{h} is a weak external input vector used to trigger the response of the population activity. Introducing n replicated dynamical states $\{\mathbf{x}^a\}_{a=1}^n$, one can calculate the quenched average of the replicated partition function as follows,

$$\begin{aligned} \langle Z_\ell^n \rangle &= \left\langle \int d\mathbf{x} \exp \left[-\beta \left(\frac{1}{2} \sum_{ia} \left(-x_i^a + \sum_j J_{ij} \phi(x_j^a) + h_i^a \right)^2 + \eta \sum_a \|\mathbf{x}^a\|^2 + \gamma \sum_{ia} \phi(x_i^a) \right) \right] \right\rangle \\ &= \left\langle \int d\mathbf{x} D\hat{\mathbf{x}} \exp \left[i\sqrt{\beta} \sum_{ia} \hat{x}_i^a \left(-x_i^a + \sum_j J_{ij} \phi(x_j^a) + h_i^a \right) - \beta\eta \sum_a \|\mathbf{x}^a\|^2 - \beta\gamma \sum_{ia} \phi(x_i^a) \right] \right\rangle, \end{aligned} \quad (\text{A37})$$

where $\langle \cdot \rangle$ indicates the disorder average over the untrained coupling and feedback weights.

Following a similar procedure as before, one obtains the free energy in the zero temperature limit.

$$-f = -\frac{1}{2} (q\hat{\chi} + 2\hat{q}\chi) + \int DuDv \mathcal{H}_0(x^*), \quad (\text{A38})$$

where $x^* = \operatorname{argmax}_x \mathcal{H}_0(x)$, and

$$\mathcal{H}_0(x) = -\eta x^2 - \gamma \phi(x) + \frac{1}{2} \hat{\chi} \phi^2(x) + \sqrt{2\hat{q}} u \phi(x) - \frac{1}{2\sigma^2} (\sqrt{g^2 q + \delta^2 q^2} v + h - x)^2. \quad (\text{A39})$$

Hence, the mean population activity $\langle \phi \rangle \equiv \frac{1}{N} \sum_i \phi_i$ can be obtained from the generating function.

$$\langle \phi \rangle = \left. \frac{\partial(-f)}{\partial(-\gamma)} \right|_{\gamma=0}. \quad (\text{A40})$$

Then the response function can be calculated by definition.

$$\begin{aligned} r &= \left. \frac{\partial \langle \phi \rangle}{\partial h} \right|_{h \rightarrow 0} = \left. \frac{\partial(-f)}{\partial h \partial(-\gamma)} \right|_{h=0, \gamma=0} \\ &= -\frac{\sqrt{g^2 q + \delta^2 q^2}}{\sigma^2} [v \phi(x^*)] + \frac{1}{\sigma^2} [x^* \phi(x^*)] - \frac{1}{\sigma^2} [x^*][\phi(x^*)]. \end{aligned} \quad (\text{A41})$$

To derive Eq. (A41), we assume a finite temperature and finally send the temperature to zero. Because of symmetry in the effective Hamiltonian, the last term in the last equality of Eq. (A41) vanishes. This response function characterizes how responsive one network state against weak external perturbations. Note that in our previous work [15], apart from the overlap matrix, there appears the other response matrix. The diagonal element is exactly the quantity r here. However, the off-diagonal element explains how two dynamical states impact each other, which may be related to psychedelics [44], but we do not attempt to discuss this phenomenon in this paper.

3. Homeostatic learning

For the homeostatic learning, the procedure of replica calculation is quite similar to that in the Hebbian learning. One distinct part arises in the quenched disorder average detailed

below.

$$\begin{aligned}
& \left\langle \exp \left[i\sqrt{\beta} \sum_{ij} J_{ij} \sum_a \hat{x}_i^a \phi(x_j^a) \right] \right\rangle \\
&= \left\langle \exp \left[i\sqrt{\beta} \sum_{ij} J_{ij}^0 \sum_a \hat{x}_i^a \phi(x_j^a) \right] \right\rangle \exp \left[-i\frac{k\sqrt{\beta}}{N} \sum_{ij} \sum_a \hat{x}_i^a \phi(x_i^a) \phi^2(x_j^a) \right. \\
&\quad \left. + \frac{i\sqrt{\beta}k}{N} r_{\text{tg}} \sum_{ij} \sum_a \hat{x}_i^a \phi^2(x_j^a) \right] \\
&= \exp \left[-\frac{1}{2} \frac{\beta g^2}{N} \sum_{ij} \left(\sum_a \hat{x}_i^a \phi(x_j^a) \right)^2 - i\frac{k\sqrt{\beta}}{N} \sum_{ij} \sum_a \hat{x}_i^a \phi(x_i^a) \phi^2(x_j^a) \right. \\
&\quad \left. + \frac{i\sqrt{\beta}k}{N} r_{\text{tg}} \sum_{ij} \sum_a \hat{x}_i^a \phi^2(x_j^a) \right] \tag{A42} \\
&= \exp \left[-\frac{1}{2} \frac{\beta g^2}{N} \sum_{ij} \sum_{ab} \hat{x}_i^a \hat{x}_i^b \phi(x_j^a) \phi(x_j^b) - i\frac{k\sqrt{\beta}}{N} \sum_{ij} \sum_a \hat{x}_i^a \phi(x_i^a) \phi^2(x_j^a) \right. \\
&\quad \left. + \frac{i\sqrt{\beta}k}{N} r_{\text{tg}} \sum_{ij} \sum_a \hat{x}_i^a \phi^2(x_j^a) \right] \\
&= \exp \left[-\frac{1}{2} \beta g^2 \sum_i \sum_{ab} \hat{x}_i^a \hat{x}_i^b Q^{ab} - ikN\sqrt{\beta} \sum_a R^a Q^{aa} + i\sqrt{\beta}kr_{\text{tg}} \sum_i \sum_a \hat{x}_i^a Q^{aa} \right].
\end{aligned}$$

The remaining steps are similar to those in Sec. A1. The final expressions of free energy in both finite and zero temperatures are summarized in the main text, together with the associated saddle-point equations in the zero temperature limit.

Appendix B: Numerical details of solving SDEs

To iteratively solve the saddle point equations, we first initialize the order parameters, and then generate $M = 100\,000$ Monte Carlo samples and identify the global maximum of $\mathcal{H}_0(x)$, i.e., x^* for each pair of (u, v) samples. Then we update the order parameters according to the following procedure until the convergence (i.e., $|\mathcal{O}_{t+1} - \mathcal{O}_t| < 10^{-3}$) is achieved. To speed up convergence, we use the following damping step:

$$\mathcal{O}_{t+1} = \alpha \mathcal{O}_t + (1 - \alpha) f(\mathcal{O}_t), \tag{B1}$$

Here, $\alpha = 0.2$ is the damping parameter. The pseudocode is given in Algorithm 1. In practice, we also use the convergent order parameters at a smaller value of g to initialize

the iteration of the SDEs for a larger value of g . This trick is useful to mitigate numerical instability.

Algorithm 1 SDE solver

Input: g , initial values of $\mathcal{O} \in \{q, \chi, r\}$ and a damping factor α

Output: convergent values of \mathcal{O}

1: **repeat**

2: generate Gaussian samples u, v

3: find x^* by the golden section search for the function $\mathcal{H}_0(x)$

4: calculate the average $[\cdot]$

5: $\mathcal{O}_{t+1} \leftarrow \alpha \mathcal{O}_t + (1 - \alpha) f(\mathcal{O}_t)$, where $f(\mathcal{O})$ is the right hand side of the saddle-point equations
 (see the main text)

6: **until** convergence

-
- [1] Mikhail I. Rabinovich, Pablo Varona, Allen I. Selverston, and Henry D. I. Abarbanel. Dynamical principles in neuroscience. *Rev. Mod. Phys.*, 78:1213–1265, 2006.
 - [2] Wulfram Gerstner, Werner M. Kistler, Richard Naud, and Liam Paninski. *Neuronal Dynamics: From Single Neurons to Networks and Models of Cognition*. Cambridge University Press, United Kingdom, 2014.
 - [3] A. Levina, J. M. Herrmann, and T. Geisel. Dynamical synapses causing self-organized criticality in neural networks. *Nature Physics*, 3(12):857–860, 2007.
 - [4] Jeffrey C. Magee and Christine Grienberger. Synaptic plasticity forms and functions. *Annual Review of Neuroscience*, 43(Volume 43, 2020):95–117, 2020.
 - [5] L. F. Abbott and Sacha B. Nelson. Synaptic plasticity: taming the beast. *Nature Neuroscience*, 3(11):1178–1183, 2000.
 - [6] Shun-ichi Amari. Dynamics of pattern formation in lateral-inhibition type neural fields. *Biological Cybernetics*, 27(2):77–87, 1977.
 - [7] Hugh R. Wilson and Jack D. Cowan. Excitatory and inhibitory interactions in localized populations of model neurons. *Biophysical Journal*, 12(1):1–24, 1972.

- [8] Haiping Huang. Eight challenges in developing theory of intelligence. *Front. Comput. Neurosci*, 18:1388166, 2024.
- [9] C. De Dominicis. Dynamics as a substitute for replicas in systems with quenched random impurities. *Phys. Rev. B*, 18:4913–4919, 1978.
- [10] Hans-Jürgen Sommers. Path-integral approach to ising spin-glass dynamics. *Phys. Rev. Lett.*, 58:1268–1271, 1987.
- [11] A. Crisanti and H. Sompolinsky. Dynamics of spin systems with randomly asymmetric bonds: Langevin dynamics and a spherical model. *Phys. Rev. A*, 36:4922–4939, 1987.
- [12] R W Penney, A C C Coolen, and D Sherrington. Coupled dynamics of fast spins and slow interactions in neural networks and spin systems. *Journal of Physics A: Mathematical and General*, 26(15):3681, 1993.
- [13] R Penney and D Sherrington. Slow interaction dynamics in spin-glass models. *Journal of Physics A: Mathematical and General*, 27(12):4027, 1994.
- [14] H. Sompolinsky, A. Crisanti, and H. J. Sommers. Chaos in random neural networks. *Phys. Rev. Lett.*, 61:259–262, 1988.
- [15] Junbin Qiu and Haiping Huang. An optimization-based equilibrium measure describing fixed points of non-equilibrium dynamics: application to the edge of chaos. *Communications in Theoretical Physics*, 77(3):035601, 2025.
- [16] Gilles Wainrib and Jonathan Touboul. Topological and dynamical complexity of random neural networks. *Phys. Rev. Lett.*, 110:118101, 2013.
- [17] Jakob Stubenrauch, Christian Keup, Anno C. Kurth, Moritz Helias, and Alexander van Mee-gen. The distribution of unstable fixed points in chaotic neural networks. *arXiv:2210.07877*, 2022.
- [18] Shishe Wang and Haiping Huang. How high dimensional neural dynamics are confined in phase space. *arXiv:2410.19348*, 2024.
- [19] Friedrich Schuessler, Alexis Dubreuil, Francesca Mastrogiuseppe, Srdjan Ostojic, and Omri Barak. Dynamics of random recurrent networks with correlated low-rank structure. *Phys. Rev. Res.*, 2:013111, 2020.
- [20] Jonas Stapmanns, Tobias Kuhn, David Dahmen, Thomas Luu, Carsten Honerkamp, and Moritz Helias. Self-consistent formulations for stochastic nonlinear neuronal dynamics. *Phys. Rev. E*, 101:042124, 2020.

- [21] Jimmy Ba, Geoffrey E Hinton, Volodymyr Mnih, Joel Z Leibo, and Catalin Ionescu. Using fast weights to attend to the recent past. In D. Lee, M. Sugiyama, U. Luxburg, I. Guyon, and R. Garnett, editors, *Advances in Neural Information Processing Systems*, volume 29. Curran Associates, Inc., 2016.
- [22] Samantha J Fournier and Pierfrancesco Urbani. Statistical physics of learning in high-dimensional chaotic systems. *Journal of Statistical Mechanics: Theory and Experiment*, 2023(11):113301, 2023.
- [23] Friedrich Schuessler, Francesca Mastrogiuseppe, Alexis Dubreuil, Srdjan Ostojic, and Omri Barak. The interplay between randomness and structure during learning in rnns. In H. Larochelle, M. Ranzato, R. Hadsell, M.F. Balcan, and H. Lin, editors, *Advances in Neural Information Processing Systems*, volume 33, pages 13352–13362. Curran Associates, Inc., 2020.
- [24] Zijian Jiang, Ziming Chen, Tianqi Hou, and Haiping Huang. Spectrum of non-hermitian deep-hebbian neural networks. *Phys. Rev. Res.*, 5:013090, 2023.
- [25] David G. Clark and L. F. Abbott. Theory of coupled neuronal-synaptic dynamics. *Phys. Rev. X*, 14:021001, 2024.
- [26] Ulises Pereira-Obilinovic, Johnatan Aljadeff, and Nicolas Brunel. Forgetting leads to chaos in attractor networks. *Phys. Rev. X*, 13:011009, 2023.
- [27] David Sussillo and L.F. Abbott. Transferring learning from external to internal weights in echo-state networks with sparse connectivity. *PLOS ONE*, 7(5), 05 2012.
- [28] Kenneth D. Miller and David J. C. MacKay. The Role of Constraints in Hebbian Learning. *Neural Computation*, 6(1):100–126, 1994.
- [29] Richard Kempter, Wulfram Gerstner, and J. Leo van Hemmen. Hebbian learning and spiking neurons. *Phys. Rev. E*, 59:4498–4514, 1999.
- [30] Gina G Turrigiano. Homeostatic plasticity in neuronal networks: the more things change, the more they stay the same. *Trends in Neurosciences*, 22(5):221–227, 1999.
- [31] Saray Soldado-Magraner, Michael J. Seay, Rodrigo Laje, and Dean V. Buonomano. Paradoxical self-sustained dynamics emerge from orchestrated excitatory and inhibitory homeostatic plasticity rules. *Proceedings of the National Academy of Sciences*, 119(43):e2200621119, 2022.
- [32] Keith B. Hengen, Alejandro Torrado Pacheco, James N. McGregor, Stephen D. Van Hooser, and Gina G. Turrigiano. Neuronal firing rate homeostasis is inhibited by sleep and promoted

- by wake. *Cell*, 165(1):180–191, 2016.
- [33] Wenxuan Zou and Haiping Huang. Introduction to dynamical mean-field theory of randomly connected neural networks with bidirectionally correlated couplings. *SciPost Phys. Lect. Notes*, page 79, 2024.
- [34] John A Hertz, Yasser Roudi, and Peter Sollich. Path integral methods for the dynamics of stochastic and disordered systems. *Journal of Physics A: Mathematical and Theoretical*, 50(3):033001, 2017.
- [35] Carson C. Chow and Michael A. Buice. Path integral methods for stochastic differential equations. *The Journal of Mathematical Neuroscience (JMN)*, 5(1):8, 2015.
- [36] David Sussillo and L.F. Abbott. Generating coherent patterns of activity from chaotic neural networks. *Neuron*, 63(4):544–557, 2009.
- [37] M. Mézard and A. Montanari. *Information, Physics, and Computation*. Oxford University Press, Oxford, 2009.
- [38] M. Mézard, G. Parisi, and M. A. Virasoro. *Spin Glass Theory and Beyond*. World Scientific, Singapore, 1987.
- [39] Haiping Huang. *Statistical Mechanics of Neural Networks*. Springer, Singapore, 2022.
- [40] Giorgio Parisi and Tommaso Rizzo. Large deviations in the free energy of mean-field spin glasses. *Phys. Rev. Lett.*, 101:117205, 2008.
- [41] Chris G. Langton. Computation at the edge of chaos: Phase transitions and emergent computation. *Physica D: Nonlinear Phenomena*, 42(1):12–37, 1990.
- [42] Nils Bertschinger and Thomas Natschläger. Real-time computation at the edge of chaos in recurrent neural networks. *Neural computation*, 16(7):1413–1436, 2004.
- [43] Dean V. Buonomano and Wolfgang Maass. State-dependent computations: spatiotemporal processing in cortical networks. *Nature Reviews Neuroscience*, 10(2):113–125, 2009.
- [44] Giulio Ruffini, Edmundo Lopez-Sola, Jakub Vohryzek, and Roser Sanchez-Todo. Neural geometrodynamics, complexity, and plasticity: A psychedelics perspective. *Entropy*, 26(1), 2024.